Polarized ^{129}Xe optical pumping/spin exchange and delivery system for magnetic resonance spectroscopy and imaging studies

M. S. Rosen,[a] T. E. Chupp, K. P. Coulter, and R. C. Welsh
Department of Physics, The University of Michigan, Ann Arbor, Michigan 48109

S. D. Swanson
Department of Radiology, The University of Michigan, Ann Arbor, Michigan 48109

(Received 1 July 1998; accepted for publication 13 November 1998)

We describe the design and construction of a laser-polarized ^{129}Xe production and delivery system that is used in our *in vitro* and *in vivo* magnetic resonance imaging (MRI) experiments. The entire apparatus including lasers and optics, rapidly actuated valves, heating and cooling, and transport tubing lies in the high magnetic field environment of a 2 T MRI magnet. With approximately 7.5% ^{129}Xe polarization, 157 cc atm of xenon gas is produced and stored as xenon ice every 5 min. Large quantities of polarized ^{129}Xe can be obtained by cycling this process. The xenon is subsequently delivered in a controlled fashion to a sample or subject. With this device we have established the feasibility of using laser-polarized ^{129}Xe as a magnetic tracer in MRI. This reliable, effective, and relatively simple production method for large volumes of ^{129}Xe can be applied to other areas of research involving the use of laser-polarized noble gases. © *1999 American Institute of Physics.* [S0034-6748(99)04802-9]

I. INTRODUCTION

In the past two decades, nuclear magnetic resonance (NMR) techniques have led to the development of magnetic resonance imaging (MRI), a very powerful, noninvasive diagnostic and research technique in medicine.[1] NMR detects precessing nuclear moments, and the NMR signal per unit volume is proportional to the nuclear magnetization $\rho\mu P$, where ρ is the density, μ is the nuclear magnetic moment, and P is the nuclear polarization. MRI exploits the variations in density and magnetic properties of these nuclear moments to produce high resolution images. Conventional MRI relies on large, static magnetic fields to produce a Boltzmann polarization of water protons that is 7×10^{-6} at 2 T. Optical pumping/spin exchange (i.e., ''laser polarization'') techniques[2] produce nonequilibrium nuclear polarization of noble gas isotopes (e.g., ^{3}He, ^{129}Xe) of order 0.1 to unity. The magnetization of these laser-polarized noble gases can be comparable to or greater than that of water protons. The use of polarized noble gases as the imaged species presents new MRI and NMR possibilities.[3–11]

The field of NMR imaging of optically polarized noble gases began with ^{129}Xe images of excised mouse lung.[12] A few milliliters of laser-polarized ^{129}Xe were used to demonstrate imaging of a laser-polarized gas in the airspaces of an *ex vivo* biological system. Laser-polarized ^{129}Xe has subsequently been used as an *in vivo* magnetic tracer,[7] providing an enhancement to currently existing MRI techniques. Laser-polarized ^{129}Xe is inhaled, and transported via blood flow where it is detected using MR spectroscopy and imaging techniques. The time-dependent, spatial distribution of ^{129}Xe signal intensity reflects local blood volume, blood flow rates, and the efficiency of perfusion and diffusive transport in tissues.

Spin-exchange optical pumping[13–17] produces highly polarized noble gases samples. In this process, a vapor of alkali metal, typically Rb, is polarized via depopulation optical pumping (Fig. 1). Circularly polarized light ($\sigma+$) excites the $D1$ transition (795 nm in Rb) from the $m_J=-1/2$ ground state to the $m_J=+1/2$ excited state. The excited state decays, or collisionally deexcites to the ground state. When the rates of optical pumping ($\gamma_{\rm opt}$) and deexcitation are high compared to the electron spin-relaxation rate ($\Gamma_{\rm SD}$) between ground state sublevels (''spin destruction''), the $m_J=-1/2$ ground state sublevel is depopulated and significant ground state Rb polarization results,

$$P_{\rm Rb}=\frac{\gamma_{\rm opt}}{\Gamma_{\rm SD}+\gamma_{\rm opt}}. \tag{1}$$

Spin exchange, mediated by the hyperfine interaction between the alkali-metal valence electron and the noble gas nucleus, can produce nearly complete nuclear polarization of noble gas samples. The Rb–^{129}Xe spin-exchange rate $\gamma_{\rm SE}=\kappa_{\rm SE}[{\rm Rb}]$. $\kappa_{\rm SE}$, the velocity-averaged binary spin-exchange cross section, is[18] $(3.7\pm0.6)\times10^{-16}\,{\rm cm}^3\,{\rm s}^{-1}$, and [Rb] is the number density of Rb atoms. The ^{129}Xe nuclear spin polarization after a polarizing time t is

$$P_{\rm Xe}(t)=\frac{\gamma_{\rm SE}}{\gamma_{\rm SE}+\Gamma_{\rm wall}}P_{\rm Rb}(1-e^{-(\gamma_{\rm SE}+\Gamma)t}), \tag{2}$$

where $\Gamma_{\rm wall}$ is the ^{129}Xe nuclear spin-relaxation rate due to interactions at the wall. From Eq. (2), the equilibrium ^{129}Xe polarization of $P_{\rm Xe}^{\infty}=\gamma_{\rm SE}P_{\rm Rb}/(\gamma_{\rm SE}+\Gamma_{\rm wall})$ and a polarization (''spin-up'') time of $T_{\rm spin\ up}=(\gamma_{\rm SE}+\Gamma_{\rm wall})^{-1}$. The application of inexpensive laser diode arrays (LDAs) to spin-

[a]To whom correspondence should be addressed; electronic mail: rosenm@umich.edu

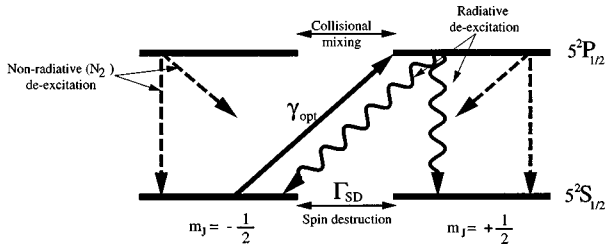

FIG. 1. Optical pumping in Rb. The nuclear spin has been neglected and the relevant states are $S_{1/2}$ and $P_{1/2}$. Incident $\sigma+$ light can only be absorbed by the $m_j=-1/2$ state which is depopulated. Due to buffer gas collisions the $P_{1/2}$ states are randomized and the probability for decay to either ground state is 1/2. The Rb resonance linewidth is 15–65 GHz, greater than the hyperfine and Zeeman splittings.

exchange optical pumping[19] has enabled increased production rates and quantities of polarized noble gas.

II. SYSTEM DESCRIPTION

Our polarized ^{129}Xe optical pumping/spin-exchange and delivery system interfaces with a conventional MRI scanner. It can produce, accumulate, and deliver large volumes of polarized ^{129}Xe to a small animal in controlled, single breath doses at high polarization *in situ*. Additionally, this system can be used to produce and deliver polarized ^{129}Xe for NMR studies of surfaces and bulk materials. A schematic of the apparatus is shown in Fig. 2. The optical pumping/delivery system is situated in the axial fringe field of the 2 T solenoidal, superconducting, horizontal-bore MRI magnet (Oxford Instruments, England).

A. Optical pumping/spin exchange

The optical pumping/spin-exchange (OPSE) cells are 17 cm long, 25 mm inner diameter Pyrex cylinders (75 cc volume) with flat end windows. A Pyrex sidearm for Rb loading is attached to the center of the cell, transverse to the plane of the valves. A Pyrex outer jacket serves as an oven. Two glass high vacuum valves (Chemglass, Inc., Vineland, NJ) are mounted transverse to the long axis near each end of the cell. These valves permit the cell to be evacuated and filled at one end and polarized Xe to be delivered at the other end. The cell is chemically cleaned[20] and internally coated[21] with octadecyltrichlorosilane (OTS) to minimize depolarizing ^{129}Xe-wall interactions.[22] The cell is placed on a turbomolecular pumping manifold, and a Rb ampoule is placed in the sidearm and sealed. The valve to the pumping station is opened, and the cell is baked out at 150 °C until the pressure equilibrates (typically 24–36 h). The bakeout is then stopped, and Rb is chased with a cool flame from the sidearm into the pumping cell. The sidearm is then pulled off with a torch. The flame never contacts any coated surface in order to avoid burning the OTS. For this reason, care must be taken during the coating process to keep OTS out of the sidearm. The cell is pumped down to final pressure of 2×10^{-8} Torr. Once produced, the optical pumping cell is backfilled to atmospheric pressure with clean N_2 and mated to the optical pumping/delivery system.

The magnetic holding field for optical pumping is provided by the 2 T magnet fringe field. In our setup the magnetic field at the cell is approximately 400 G. This field is oriented predominately along the long axis of the OPSE cell. A Hemholtz coil pair would also produce a suitable magnetic field, allowing the apparatus to be set up in a magnetic field-free enviornment. The ^{129}Xe relaxation rate in OTS coated cells (Γ_{wall}) is strongly dependent on magnetic field.[22] The spin-exchange rate γ_{SE} varies from $5\times10^{-4}\,s^{-1}$ at 80 °C to $7\times10^{-3}\,s^{-1}$ at 120 °C. A magnetic field of greater than 20 G at the OPSE cell results in $\Gamma_{wall}\ll\gamma_{SE}$ over this temperature range. The contribution to ^{129}Xe relaxation in the pump cell due to magnetic-field inhomogeneities can be estimated[23] from $\Gamma_{\nabla B}=(|\nabla B_\perp|^2D)/B_0^2$, where $B_\perp$ is the transverse component of the magnetic-field inhomogeneity, B_0 is the longitudinal magnetic holding field, and D is the xenon diffusion

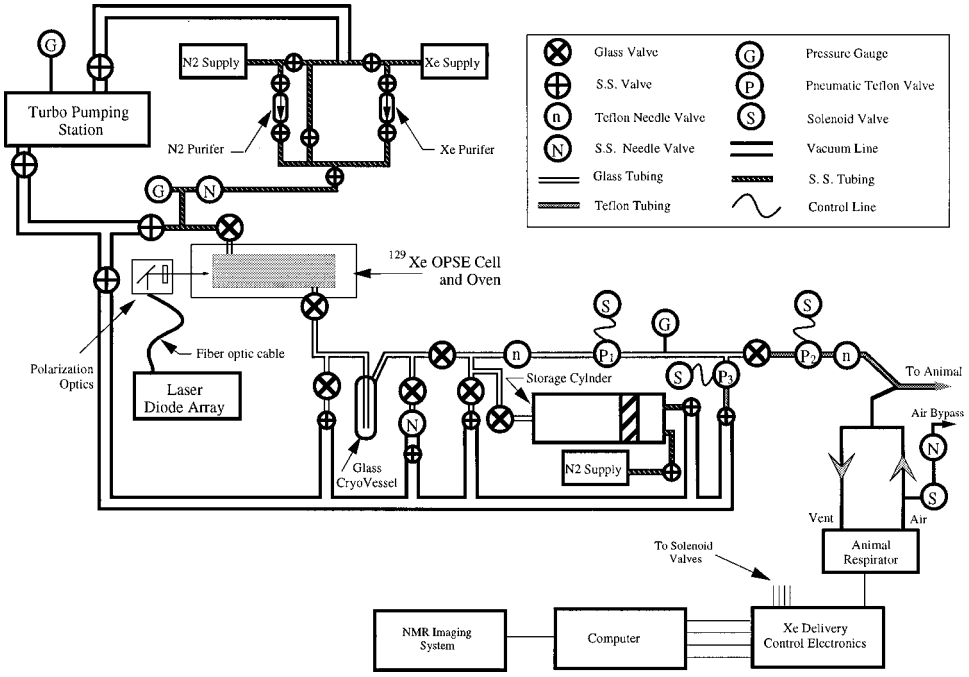

FIG. 2. Schematic of the optical pumping/spin-exchange and delivery system.

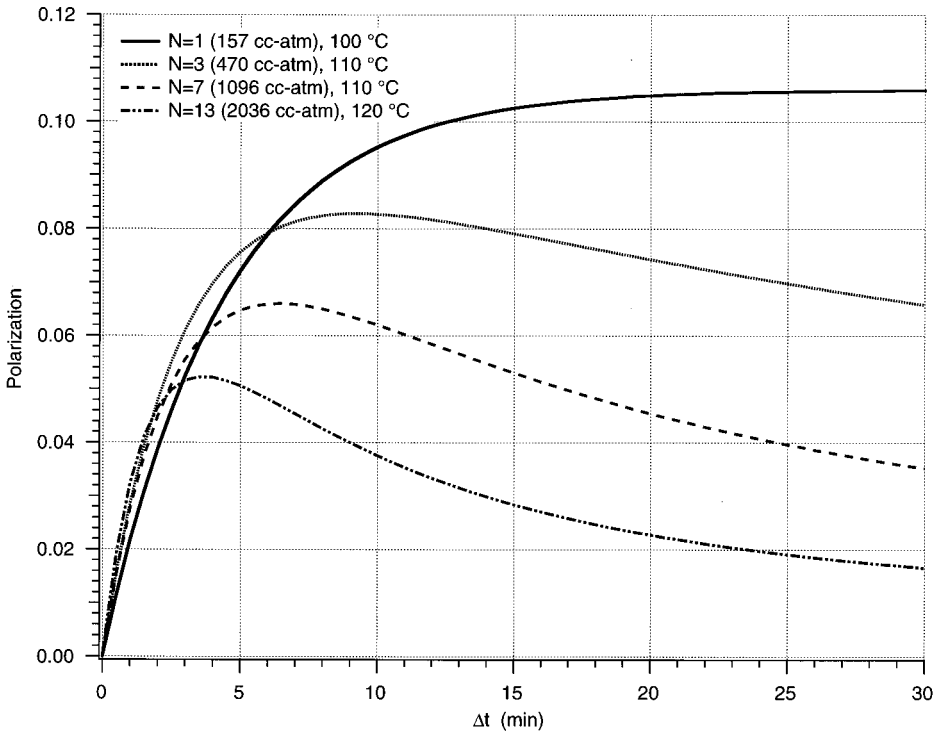

FIG. 3. Calculations of P_{Final}, the polarization of frozen ^{129}Xe after N accumulation cycles, as a function of polarizing time, Δt. The total accumulation time is thus $N\Delta t$. The laser power, OPSE cell geometry, and gas pressures are as described in the text, with $T_1^{\text{ice}}=3600$ s. Note that the Δt for which P_{Final} is maximal decreases with increasing N. The cell temperature, T, indicated for each curve has been chosen to maximum P_{Final}. This optimum T for each curve also increases with N.

constant. Requiring $\Gamma_{\nabla B} \ll \gamma_{\text{SE}}$, transverse magnetic gradients of less than 5% are suitable under most conditions. Hot air (typically 80–120 °C) flowing through the OPSE cell oven maintains an adequate Rb vapor density (typically 10^{12}–$10^{13}\,\text{cm}^{-3}$). For each experiment, the OPSE cell is filled with 1700 Torr of highly purified (Ultrapure Systems, Colorado Springs, CO) natural xenon (26.4% ^{129}Xe). Matching the Rb vapor density to the available laser power maximizes the optical pumping efficiency. Optimization of the OPSE parameters is discussed below. 150 Torr of N_2 suppresses radiation trapping[17] in the pumping cell. Two fiber-coupled LDAs (Opto Power, Tuscon, AZ) each provide 15 W of cw laser light with a 2–3 nm full width at half maximum (FWHM). The LDA light is circularly polarized and incident on the OPSE cell.

B. Xe transport manifold

Once polarized, the ^{129}Xe is allowed to expand from the optical pumping cell into the transport manifold for accumulation, storage, and eventual delivery to the subject or sample. It is necessary that all materials in the system be compatible with the transport of polarized ^{129}Xe and be suitable for use in the high field environment near the MRI magnet. Contaminants that depolarize ^{129}Xe (such as paramagnetic O_2) are minimized. This necessitates the use of ultrahigh vacuum (UHV) techniques. Many of the components typically used in UHV systems, such as stainless-steel valves and tubing, depolarize ^{129}Xe. Glass isolation valves are placed between polarized ^{129}Xe in the manifold and each UHV valve. These valves are kept closed when polarized gas is being transported and are operated in conjunction with the UHV valves when pumping out the manifold. The bulk of the manifold is constructed out of Pyrex with individual substructures (such as the OPSE cell) mating to the manifold via Teflon unions (Swagelok, Hudson, OH).

C. Polarized ^{129}Xe accumulation

A batch mode production method accumulates large volumes of polarized ^{129}Xe. This method exploits the long lifetimes of ^{129}Xe in the OTS-coated OPSE cell (600–800 s) and the extremely long lifetimes achievable in frozen[24] state. The strong magnetic-field dependence of the ice relaxation rate becomes essentially independent of magnetic-field strength at fields above 500 G. The magnetic field at the ice storage cell is 500 G, resulting in a ^{129}Xe ice relaxation time (T_1^{ice}) at 77 K on the order of 1 h. Significantly longer relaxation times are obtained at lower temperatures. In low magnetic-field applications, this field is provided by a permanent magnet.[25] The polarized gas mixture is pumped from the OPSE cell through the evacuated ice storage cell. The ice storage cell is a 5 cc OTS-coated Pyrex trap immersed in LN_2. Xe freezes and remains in the storage cell while the N_2 is pumped away. Cryotrapping[26] occurs in mixtures of condensable and noncondensable gases and can prevent complete Xe accumulation. The geometry of the freezing cell and the turbulent flow of gas through it minimizes cryotrapping. Additionally, the pumping of the hot gas mixture from the OPSE cell through the cryogenic trap cools the gas and reduces the Rb vapor pressure. This prevents Rb vapor from being delivered to the subject or sample. The polarization/accumulation cycle is repeated to accumulate additional Xe as ice.

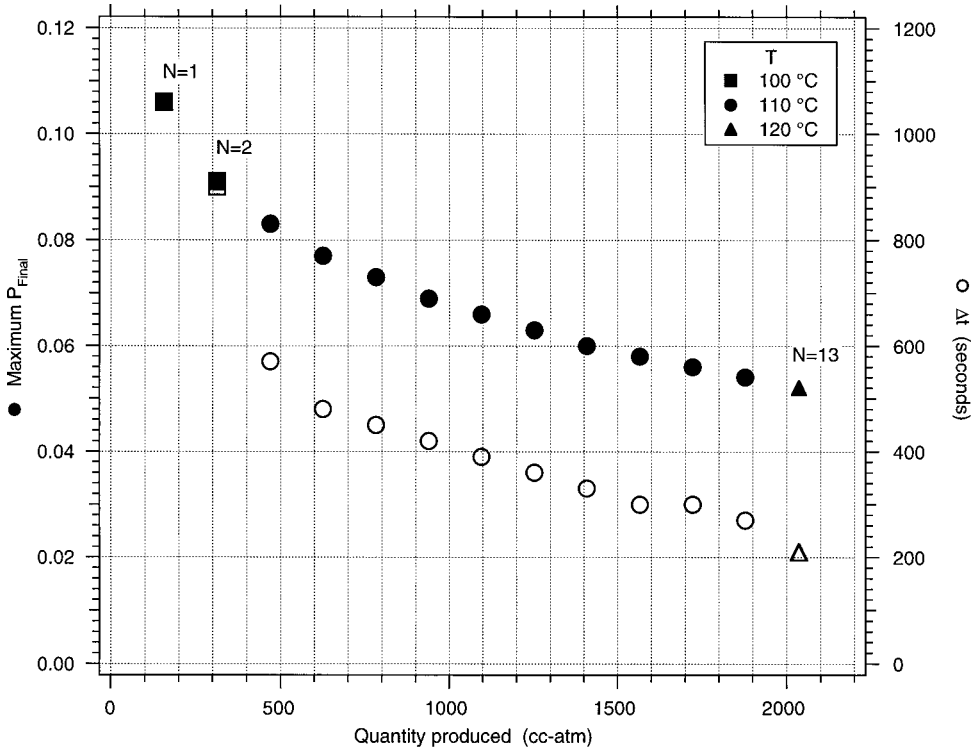

FIG. 4. Calculation of the maximum ^{129}Xe polarization attainable with $T_1^{ice}=3600$ s. The final polarization at the end of N accumulation cycles is shown as a function of the ^{129}Xe volume produced. The corresponding Δt for each N is also shown. The OPSE parameters (T and Δt) for each N have been individually optimized to maximize the Xe polarization. A single cycle ($N=1$) asymptotically approaches P_{Final} (Fig. 3), and hence no Δt is given.

D. Polarized ^{129}Xe gas storage

Once a sufficient volume of ^{129}Xe has been accumulated in the solid phase, it is expanded for subsequent delivery to the subject or sample. The polarized gas storage system provides a constant pressure polarized ^{129}Xe source. The gas storage cell is a precision bore, 7.6 cm diameter, 25 cm long Pyrex cylinder internally coated with OTS. A Teflon piston fits inside this cylinder and provides a gas-tight seal. The gas storage assembly resembles a large syringe. The cylinder is mated to 6 mm Pyrex tube at one end and a plastic cap provides a leak-tight seal to the other end. The cylinder is evacuated and pressurized through the 6 mm Pyrex tube via the ^{129}Xe transport manifold. The space behind the piston is pressurized or evacuated via a connection in the plastic cap. The piston is initially located at the back of the cylinder. The 1 ℓ cylinder volume is subsequently evacuated via the gas transport manifold. The Xe cryovessel is rapidly thawed, and the gas freely expands into the storage cylinder. The valve between the cryovessel and the syringe is closed and a N_2 source provides back pressure to the piston producing a constant pressure polarized ^{129}Xe source for the delivery system. The ^{129}Xe gas polarization lifetime (T_1) is 18 min in the ''syringe,'' with no observed dependence on the position of the piston in the cylinder (i.e., the surface-to-volume ratio).

E. Polarized ^{129}Xe delivery

At the conclusion of the accumulation cycle, the syringe contains polarized ^{129}Xe gas which must be delivered to the subject or sample (located in the center of the NMR magnet) in a controlled manner and with a minimal loss of polarization. The absence of large transverse magnetic field gradients minimizes ^{129}Xe depolarization during transport from the system to the subject; atoms adiabatically follow the local direction of the magnetic field. Control of remotely activated valves allows complete automation of the delivery cycle, and is optimized for a particular application by the specific programming of the control electronics or computer. The polarized gas delivery system transports polarized ^{129}Xe continuously at a fixed rate or in metered volumes, either to a sample or in single breath doses to an animal subject. The repeated delivery of small volumes of polarized gas to an animal subject allows averaging of signals over repeated inhalations and systematic studies *in vivo*. The xenon flows from the gas storage system to the sample or animal without coming in contact with oxygen. This is critical to ensure low loss of ^{129}Xe polarization. For *in vivo* work, O_2 is precisely mixed with (Fig. 2) Xe at the animal interface via the air bypass needle valve. *In vitro* work can be done completely excluding O_2.

A Teflon-stem needle valve (Chemglass, Vineland, NJ) provides a variable gas conductance between the Xe ''syringe'' and the gas delivery system. This valve is adjusted to match the rate of gas flow to the speed of the automated valves. The volume between the pneumatically actuated Teflon valves (Teqcom Industries, Santa Ana, CA), P_1 and P_2, serves as a *ballast volume*. P_1 is mated to the glass transport manifold, and P_2 is an integral part of the experimental platform containing NMR probe and the sample or subject. P_2 mates to a Teflon PFA (Swagelok, Hudson, OH) plug valve on the delivery system via PFA tubing. This flexible tubing is minimally depolarizing, and the ease of connection to the system allows for rapid removal and installation of the experimental platform in the magnet. All the pneumatic valves are controlled via solenoidal valves (S_i) outside the high magnetic-field environment of the NMR magnet. These solenoidal valves are driven by the control electronics. A nonmagnetic pressure transducer (Honeywell Microswitch, Free-

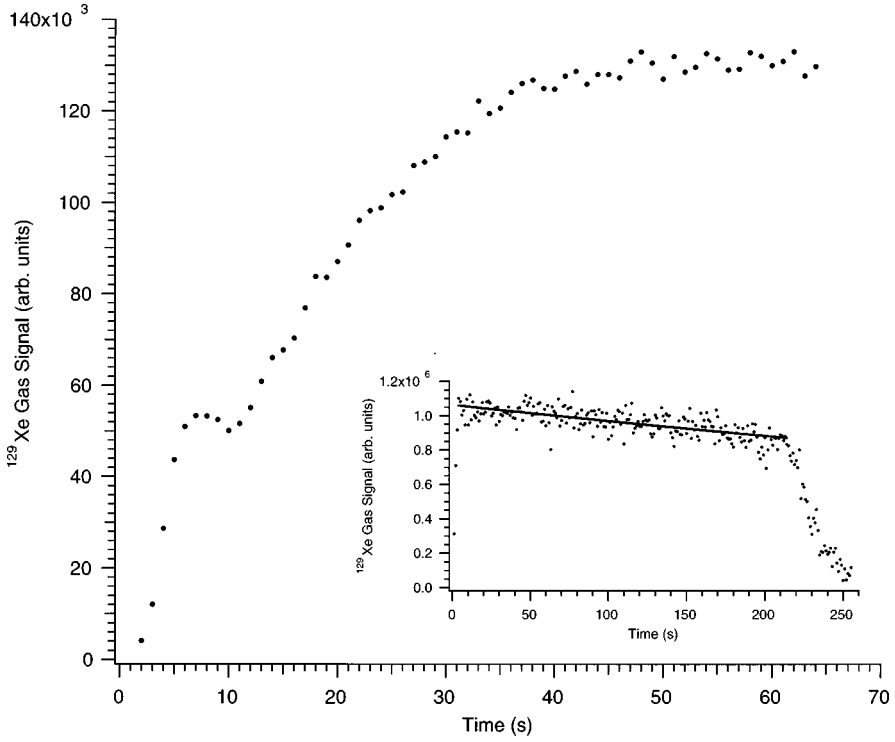

FIG. 5. Magnitude of ^{129}Xe gas spectrum vs time acquired from a surface coil placed on the rat thorax. The rat was ventillated with 60% Xe/40% O_2 (2.2 cc/breath total) at 80 breaths per minute. Spectra were acquired every 500 ms. NMR acquisition was triggered by delivery valve P_2. Inset: Magnitude of ^{129}Xe gas spectrum vs. time acquired from a volume probe around a 0.7 cc glass vial. 1.2 cc ($\pm$5%) of ^{129}Xe was delivered every second for 220 s. 256 spectra were acquired with a nominal 25° tip angle. A fit of a single exponential to this range yields a ''syringe'' T_1 of 1076$\pm$71 s. The signal decreases rapidly after delivery was stopped, due to repeated 25° tips of the same gas.

port, IL) mounts into the glass transport manifold via an O-ring seal and continuously monitors the pressure of the ballast volume. The control electronics fill the ballast volume with polarized ^{129}Xe to a set pressure and deliver each bolus of polarized ^{129}Xe directly to the sample or subject. The control electronics package consists of circuitry which monitors the ballast volume pressure and allows for the setting of gas delivery volume and gas delivery timing for valve actuation and cycle synchronization. The electronics are programmed for repeated filling and emptying of a NMR sample with polarized ^{129}Xe or delivery to living animals.

III. EXPERIMENTAL RESULTS AND DISCUSSION

After a polarizing time Δt, the polarization in the OPSE cell is [from Eq. (2)]

$$P_{\mathrm{Xe}}(\Delta t)=P_{\mathrm{Xe}}^{\infty}(1-e^{-\Delta t/T_{\mathrm{spinup}}}). \tag{3}$$

After N accumulation cycles (i.e., a total time of $N\Delta t$), the polarization of the ^{129}Xe ice is

$$P_{\mathrm{Final}}(N\Delta t)=\frac{P_{\mathrm{Xe}}(\Delta t)}{N}\sum_{m=1}^{N} e^{[-\Delta t(m-1)]/T_1^{\mathrm{ice}}}. \tag{4}$$

The final polarization of the ^{129}Xe for a desired volume can be maximized by appropriate choice of P_{Xe}^{∞}, T_{spinup}, and Δt. P_{Xe}^{∞} can be computed[19] over a range of Xe pressure and cell temperature (T) for a given cell geometry and laser spectral profile. The optimal values for the parameters T and Δt are then found by maximizing P_{Final}, the maximum attainable ^{129}Xe polarization. In our experiments, the OPSE cell is filled with 1700 Torr of Xe, resulting in 157 cc atm of Xe polarized per OPSE cycle. If a small volume of polarized Xe is desired, the total number (N) of OPSE cycles is small. The ^{129}Xe polarization loss due to T_1^{ice} is neglible since the total time $N\Delta t \ll T_1^{\mathrm{ice}}$. Thus, P_{Final} is optimized with a longer Δt. Larger volumes of ^{129}Xe require more OPSE cycles, resulting in a longer total accumulation time, $N\Delta t$. As a result, individual batches of polarized ^{129}Xe may spend a significant time in the frozen state. Thus, in order to prevent large polarization losses due to T_1^{ice}, the cycle time Δt must decrease. A sufficient increase in γ_{SE} is achieved with a corresponding increase in OPSE cell temperature. Calculations of P_{Final} as a function of Δt, for several N, are shown in Fig. 3. For a given OPSE cell (with a measured Γ_{wall}), the calculated optimal values for T and Δt agree with experiment to better than 5%; P_{Final} agrees to approximately 15%. Uncertainties in modeling the trajectory of the divergent laser beams through the OPSE cell are the dominant cause of the greater discrepancy in P_{Final}. Calculations of the maximum P_{Final} achievable with our system as a function of volume produced is shown in Fig. 4. For each N, the family of curves P_{Final} versus Δt are computed over a range of cell temperature, T. Figure 4 shows the values of T and Δt which maximize P_{Final}.

The ^{129}Xe production rate depends on the desired final polarization. A single ($N=1$) batch, polarized for $\Delta t = 5$ min results in 157 cc atm of Xe at 7.5% polarization. The polarization is measured by comparison to the thermally polarized ^{129}Xe signal, at the interface to the subject/sample. NMR spectroscopy or imaging in our small animal experiments lasts from 2 to 4 min. With a 50% Xe/50% O_2 ventilatory mixture, this requires 100 cc of polarized Xe per minute of running time. The system typically is run for $N = 3$ cycles, with $\Delta t = 5$ min. This results in 470 cc atm of Xe polarized to roughly 7.5%. In practice, however, the system cycle time is longer due to the manual operation of the valves associated with the OPSE cell, typically about 50 s per batch. Modifications to fully automate the OPSE valves and thus minimize this delay are currently underway. Thus,

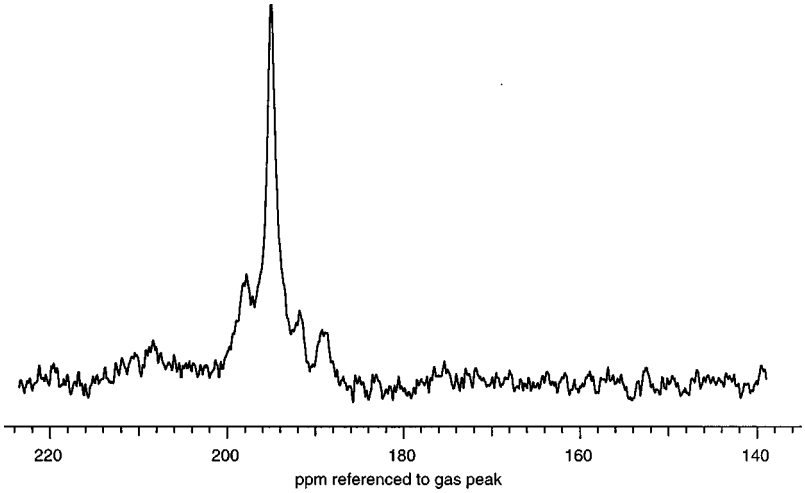

FIG. 6. NMR spectrum of laser-polarized ^{129}Xe in the rat head. The gas phase resonance is set to 0 ppm. This spectrum was acquired from 256 averages over two runs of 50 s each. Nominal 20° tip angle, 2 kHz sweep width, $T_r = 0.5$ s.

in its current configuration, 470 cc atm of Xe are produced in approximately 17.5 min to roughly 7.5% polarization.

The performance of the delivery system is illustrated in Fig. 5. The magnitude of the NMR signal in the lungs of a live rat ventillated for over 1 min with 60% Xe and 40% O_2 is shown. The Xe/O_2 mixture was delivered in 2.2 cc breaths at 80 breaths per minute. The ^{129}Xe polarization is approximately 4.5% in these experiments. The rat was located on the experimental platform at the center of the magnet. A surface coil tuned to the ^{129}Xe gas resonance was placed on chest of the animal. The ^{129}Xe signal saturates and is maintained for extended times. This constant input magnetization is essential for ^{129}Xe magnetic tracer studies.[27] We have performed *in vivo* studies with 1:1 Xe/O_2 mixture for run times exceeding 4 min with similar results.

The use of laser polarized ^{129}Xe in experiments with larger systems, particularly humans, may require greater ^{129}Xe magnetization. The limiting factor in the accumulation of multiple batches of ^{129}Xe at the single-batch polarization is clearly T_1^{ice}. Relaxation times as long as 500 h have been demonstrated[24] at 4.2 K and 1 kG, and raise the possibility of extremely long accumulation times in a liquid helium cooled cryotrap. Isotopicaly enriched ^{129}Xe can produce approximately three times greater specific magnetization, but at a significantly greater cost. In general, the polarizations, production rates, and volumes of polarized gases are limited by the available lasers. Greater ^{129}Xe polarization requires greater laser power within the Rb absorption linewidth, since $\gamma_{\text{opt}} = \int \Phi(\nu)\sigma_0(\nu)d\nu$, where $\Phi(\nu)$ is the incident photon flux per unit frequency and $\sigma_0(\nu)$ is the Rb absorbtion cross section. LDAs, although convenient and relatively inexpensive, are far from ideal light sources due to their low spectral density; in the OPSE cell, less than one watt of LDA light is absorbed. Increased spectral density leads to increases in ^{129}Xe polarization and production rate. This can be achieved with greater total LDA laser power or by using narrow band lasers, such as Ar^+/Ti:sapphire lasers.

The OPSE method described here is similar in performance to the method used in a device described by Driehuys *et al.*,[25] which polarizes a continuous gas flow of ^{129}Xe. Their device takes advantage of the broad spectral width (2–3 nm FWHM) of a very high power (140 W) LDA by collisionally broadening the Rb $D1$ absorbtion profile using a high-pressure buffer gas.

The system described here has allowed us to perform systematic studies and establish the feasibility of noble gas MRI as a magnetic tracer *in vivo*. With this apparatus, we have imaged rodent lungs *in vivo*, spectroscopically studied[27] the transport of polarized ^{129}Xe to the rat brain *in vivo* (Fig. 6), and produced the first images[7] of polarized ^{129}Xe in the brain of a living rat. We have also studied the distribution of ^{129}Xe in the entire rodent body and acquired ^{129}Xe images of blood in the heart and kidneys *in vivo*.[28] The ability to produce and repeatedly deliver small volumes of polarized gas to the animal subject allows averaging of signals over repeated inhalations and makes systematic *in vivo* studies feasible. Simple modifications will allow the system to be placed in a magnetic-field-free environment, greatly expanding research potential. In a clinical setting, we anticipate the utilization of ^{129}Xe MRI in such diverse applications as air space imaging, combined air space/tissue imaging, cardiac perfusion imaging, brain and major artery imaging, and measurement of regional cerebral blood flow.

ACKNOWLEDGMENTS

The authors wish to gratefully acknowledge Roy Wentz's glass-blowing expertise and advice. The authors thank Jon Zerger for many helpful discussions. This work was supported by the National Science Foundation and the National Institute of Health.

[1] For review see: F. W. Wehrli, Prog. Nucl. Magn. Reson. Spectrosc. **28**, 87 (1995).
[2] T. G. Walker and W. Happer, Rev. Mod. Phys. **69**, 629 (1997).
[3] X. J. Chen, M. S. Chawla, L. W. Hedlund, H. E. Moller, J. R. MacFall, and G. A. Johnson, Magn. Reson. Med. **39**, 79 (1998).
[4] E. E. de Lange, J. P. Mugler, J. R. Brookeman, T. M. Daniel, J. D. Truwitt, C. D. Teates, and J. Knight-Scott, Proceedings of the 6th Annual ISMRM Conference, Sydney, Australia, 1998.
[5] H. U. Kauczor, M. Ebert, K. F. Kreitner, H. Nilgens, R. Surkau, W. Heil, D. Hofmann, E. W. Otten, and M. Thelen, J. Magn. Res. Imag. **7**, 538 (1997).
[6] J. P. Mugler *et al.*, Magn. Reson. Med. **37**, 809 (1997).
[7] S. D. Swanson, M. S. Rosen, B. W. Agranoff, K. P. Coulter, R. C. Welsh, and T. E. Chupp, Magn. Reson. Med. **38**, 695 (1997).
[8] M. E. Wagshul, T. M. Button, H. F. Li, Z. R. Liang, C. S. Springer, K.

Zhong, and A. Wishnia, Magn. Reson. Med. **36**, 183 (1996).
[9] G. Navon, Y. Q. Song, T. Room, S. Appelt, R. E. Taylor, and A. Pines, Science **271**, 1848 (1996).
[10] E. Brunner, R. Seydoux, M. Haake, A. Pines, and J. A. Reimer, J. Am. Chem. Soc. **119**, 11711 (1997).
[11] L. Durrasse, G Guillot, P. J. Nacher, and G. Tastevin, C. R. Acad. Sci., Ser. IIb: Mec., Phys., Chim., Astron. **324**, 691 (1997).
[12] M. S. Albert, G. D. Cates, B. Driehuys, W. Happer, B. Saam, C. S. Springer, and A. Wishnia, Nature (London) **370**, 199 (1994).
[13] M. A. Bouchiat, T. R. Carver, and C. M. Varnum, Phys. Rev. Lett. **5**, 373 (1960).
[14] R. M. Herman, Phys. Rev. A **137**, 1062 (1965).
[15] B. C. Grover, Phys. Rev. Lett. **40**, 391 (1978).
[16] W. Happer, E. Miron, S. Schaefer, D. Schreiber, W. A. van Wijngaarden, and X. Zeng, Phys. Rev. A **29**, 3092 (1984).
[17] T. E. Chupp and K. P. Coulter, Phys. Rev. Lett. **55**, 1074 (1985).
[18] G. D. Cates, R. J. Fitzgerald, A. S. Barton, P. Bogorad, M. Gatzke, N. R. Newbuey, and B. Saam, Phys. Rev. A **45**, 4631 (1992).
[19] M. E. Wagshul and T. E. Chupp, Phys. Rev. A **40**, 4447 (1989).
[20] Cleaning procedure: 2 min in hot Alcanox/DI H_2O, rinse (3×) with DI H_2O; Piranah (30% H_2O_2 +97% H_2SO_4 3:7 v/v) for 1 h; rinse (3×) with DI H_2O; rinse (3×) with methanol; rinse (3×) with DI H_2O; dry in air under heatlamp or with N_2.
[21] Coating procedure: 5 min in coating solution, dry in air under heatlamp or with N_2, rinse (3×) with $CHCl_3$; bake or air dry/bake in rough vacuum at 200 °C for >16 h. Coating solution is: 2 mM (0.788 cc/ℓ) solution of OTS in 80% *n*-hexane +12% CCl_4 +8% $CHCl_3$ (v/v).
[22] B. Driehuys, G. D. Cates, and W. Happer, Phys. Rev. Lett. **74**, 4943 (1995).
[23] R. L. Gamblin and T. R. Carver, Phys. Rev. A **138**, A946 (1965).
[24] M. Gatzke, G. D. Cates, B. Driehuys, D. Fox, W. Happer, and B. Saam, Phys. Rev. Lett. **70**, 690 (1993).
[25] B. Driehuys, G. D. Cates, E. Miron, K. Sauer, D. K. Walter, and W. Happer, Appl. Phys. Lett. **69**, 1668 (1996).
[26] P. A. Redhead, J. P. Hobson, and E. V. Kornelsen, *The Physical Basis of Ultrahigh Vacuum* (American Institute of Physics, New York, 1993).
[27] K. P. Coulter, T. E. Chupp, M. S. Rosen, S. D. Swanson, and R. C. Welsh (in preparation).
[28] S. D. Swanson, M. S. Rosen, K. P. Coulter, R. C. Welsh, and T. E. Chupp, Magn. Res. Med. (submitted).